

A New Turbine-Sail Coupled Propulsive System for Autonomous Sailboats*

Jiayi Qiu², Jiafan Hou², Chongfeng Liu², Hengli Liu^{2,3}, Xiongwei Lin¹,
 Zhenglong Sun^{1,2}, Ning Ding², Tin Lun Lam^{1,2}, and Huihuan Qian^{1,2,†}

Abstract— Autonomous sailboats are good candidates to perform long-term missions in oceans since they are wind-propelled. Furthermore, wind turbine is a useful device that can provide autonomous sailboats with necessary electrical energy to support controller, drive rudder and sail. Some current applications for onboard wind turbines can reduce fuel demand of autonomous power sailboats. Apart from necessary electrical energy supply, autonomous sailboats also need enough propelling forces to move efficiently in the direction of the course.

In this paper, we propose a new turbine-sail coupled system that utilizes wind sources by adding two vertical wind turbines on both sides of the sail. Experiments are conducted in a wind tunnel. The results show that the system can increase the maximum propelling force when sailing downwind and allow further regulation of the force by slowing the rotation speed of wind turbine on one side.

I. INTRODUCTION

The demand for various Unmanned Surface Vehicles (USVs) is largely increased due to the commercial, scientific, environmental and military issues in a worldwide scope [1]. Some applications for USVs, such as anti-terror, surveillance and reconnaissance [2], surface cleaning [3] and damage detecting [4], require high flexibility of USV behaviors. These USVs are powered by engines that use batteries or fossil fuel for energy supply, which means only short-range maritime activities can be adopted considering the limited storage space and load capacity for large-scale engine or battery apparatuses onboard [5]. In order to complete long-range and long-endurance missions, USVs need to overcome the problems associated with energy supply. So, autonomous wind-driven sailboats provide a promising good solution for long-term missions, such as oceanic surveys and ocean transportation, etc.

The control strategies and path planning for autonomous sailboats have been widely studied to obtain a better performance in navigation [6]–[10]. But only a few researchers proposed innovative designs for autonomous sailboats in order to achieve favorable wind energy utilization. Wind turbine is usually used in such designs as a blade-connected generator. A hardware architecture for

*This paper is partially supported by Project U1613226 supported by NSFC, China, Robotic Discipline Development Fund (2016-1418) from Shenzhen Gov, R&D Project of Ministry of housing and urban construction (Grant No.2018-K8-034) and PF.01.000143 from the Chinese University of Hong Kong, Shenzhen.

[†]Shenzhen Institute of Artificial Intelligence and Robotics for Society.

²The Chinese University of Hong Kong, Shenzhen.

³University of Science and Technology of China.

[†]Corresponding author is Huihuan Qian, email: hhqian@cuhk.edu.cn

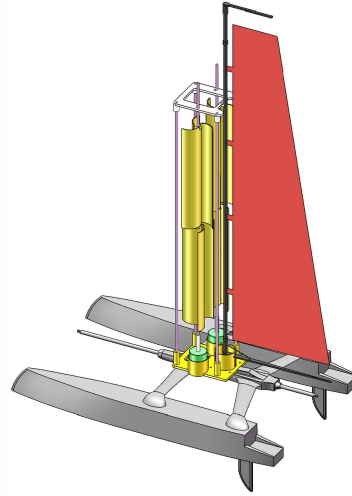


Fig. 1. A catamaran with proposed turbine-sail system.

an autonomous sailing robot was proposed by researchers from Institute for Intelligent Systems and Robotics at UPMC, which includes a wind turbine together with a solar panel to harvest wind energy and solar energy combined with a battery pack for energy autonomy [11]. A conceptual model of a hybrid electric sailboat was presented by a group from Spain, with wind turbines placed on the top of the mast or placed in the stern to provide wind power generation. The generation of other renewable energies, such as solar and hydro, are also included in the proposed model through photovoltaic panels and hydrogeneration [12]. Deserved to be mentioned, wind turbines in these researches are simply used to supply power.

In this paper, we present a turbine-sail coupled propulsive system that can utilize wind energy in two aspects: generating power and increasing propulsion. The system contains two vertical wind turbines on both sides of the sail with two boost converters respectively control the rotation speed of each wind turbine by changing the duty cycle of the circuits. Since wind turbines and sail are coupled, the forces on sail are affected. The system has been tested in a wind tunnel and the results show that when sailing downwind, the maximum propelling force is increased. Meanwhile, the rotating wind turbines can generate power in practical applications. Our results also show that by changing the difference in rotation speed between the two wind turbines, the maximum propelling force can be adjusted. This gives guidance to some sailing situations. When sailing downwind,

the sailboat can have power generation and also obtain larger propulsion. If the sailboat needs to speed up when the energy is still sufficient, it can slow down the rotation speed of the wind turbine on one side. In this case, although the power generation is reduced, the maximum propulsion force for the sailboat is increased.

This paper is organized as follows. The system design is presented in Section II, which includes the turbine-sail structure, the boost converter circuit and the automatic test platform. Two sets of experiments are described in Section III, which correspondingly tested the influence on propulsion caused by adding wind turbine blades and by adjusting rotation speed of the wind turbines. The conclusion and future works are given in Section IV.

II. PROPOSED SYSTEM

A. Turbine-Sail Structure

This structure is inspired by Bernoulli's theorem that fluid pressure decreases at points where the speed of the fluid increases, vice versa. Two vertical wind turbines are placed on each side of the sail. The airflow speed will be changed during the rotation of wind turbine blades, which will change the fluid pressure on each side of the sail. The forces on sail will be affected as a result. The design type of these vertical wind turbines is based on Savonius wind turbine. Savonius wind turbine is a vertical axis device having two half-cylindrical parts attached to the opposite sides of a vertical shaft and operated on the drag force. The concave part of the rotor blades withstands a larger drag force than the convex part when they rotate around a vertical shaft. The difference of the drag force can drive the Savonius rotor [13]. Although Savonius rotor has lower efficiency than Darrieus rotor, it requires a lower torque for start-up [14]. In order to maintain the low start-up requirement of Savonius wind rotor after combined with sail, the blades of proposed turbine-sail structure are consisted of two identical segments with three Savonius blades in each, displayed in distribution with a 60° phase difference between adjacent segments. A total of six blades in two segments are uniformly distributed over the cross-section. As shown in Figure 2, the blades are attached to a vertical shaft, which is parallel to the mast. Both the sail (mast) and the wind turbines are fixed by the support. The generators of wind turbines are placed on a lower support plate. Each generator shaft is connected to the vertical shaft of a wind turbine through a connection structure. With this connection, the generator can be driven by the rotation of vertical wind turbine blades.

B. Boost Converter and Wind Turbine Rotation Speed Adjustment

In order to adjust the rotation speed of wind turbines, boost converters are used in the proposed system. As shown in Figure 3, the boost converter consists of a transistor switch Q , which is a MOSFET, an inductor L , a diode D , and a capacitor C . When the circuit works in a continuous mode, the output voltage V_o can be calculated by Equation (1). By

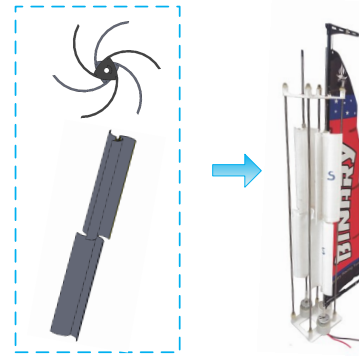


Fig. 2. The vertical wind turbine blade design and the proposed turbine-sail structure.

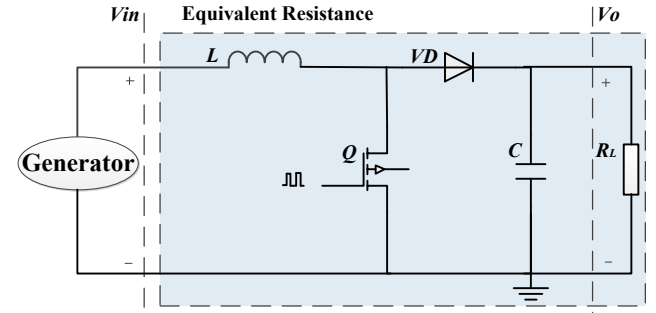


Fig. 3. The conventional boost converter and its equivalent resistance.

changing the duty cycle of the transistor switch, the output voltage can be controlled.

$$V_o = \frac{V_{in}}{1 - \alpha} \quad (1)$$

where V_{in} denotes the input voltage which is generated by the generator and α denotes the duty cycle.

When the load of the boost circuit is a resistive load and the conversion efficiency is 100%, the expression of output power is shown as Equation (2).

$$\frac{V_o^2}{R_L} = \frac{\left(\frac{V_{in}}{1-\alpha}\right)^2}{R_L} = \frac{V_{in}^2}{R_L(1-\alpha)^2} = \frac{V_{in}^2}{R_{eq}} \quad (2)$$

That is,

$$R_{eq} = (1 - \alpha)^2 R_L \quad (3)$$

where R_{eq} is the equivalent resistance, R_L is the total load resistance.

The total resistance force can be expressed as Equation (4).

$$F_t = F_f + F_e \quad (4)$$

where F_t denotes the total value of resistance force, F_f denotes the friction and F_e denotes the ampere's force.

Considering that the rotation speed of wind turbine is negatively correlated with F_t and the equivalent resistance is inversely proportional to F_e , the relationship between the

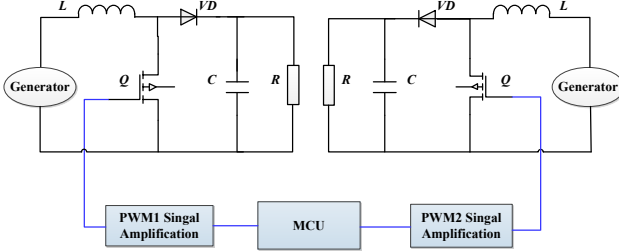


Fig. 4. Two independent PWM channels generated by Arduino to control the boost circuits on both sides.

rotation speed of wind turbine and duty cycle α can be derived as Equation (5).

$$V_{wind-turbine} \propto \frac{1}{F_t} \propto R_{eq} \propto \frac{1}{\alpha} \quad (5)$$

where $V_{wind-turbine}$ denotes the rotation speed of wind turbine.

The rotation speed $V_{wind-turbine}$ and the duty cycle α have a negative correlation. By giving different duty ratios, the equivalent resistance of boost converter on each side can be different, which means wind turbine on each side of the proposed structure can rotate at different speeds. As shown in Figure 4, two boost converters are controlled by two independent channels of Pulse Width Modulation (PWM) signals generated by the microcontroller unit (MCU). The PWM signals generated by the MCU are amplified to match the Boost converter circuits. Thus, the rotation speeds of two wind turbines can be regulated only by changing the duty cycles of PWM signals.

C. Automatic Test Platform

In order to collect the data of forces on sail at different angles of attack, the turbine-sail structure is rotatable in a wind field with constant wind direction. An automatic test platform is built to achieve precise rotary positioning as well as high efficiency in experiments. Forces data is collected at different rotation angles. As shown in Figure 5, a stepper

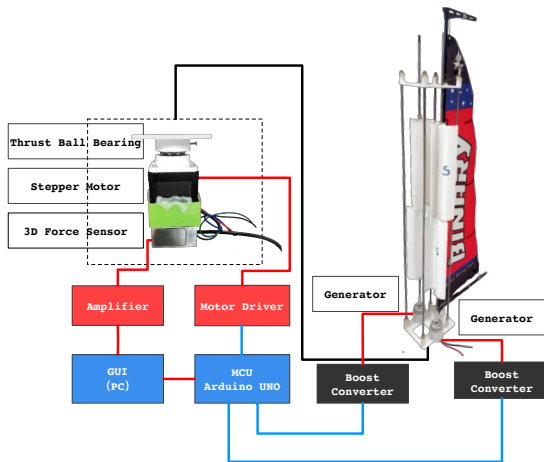


Fig. 5. Structure and control design of automatic test platform.

motor is attached above a three-dimensional force sensor. A thrust ball bearing is added to the output shaft of the stepper motor and fixed under the lower support for the turbine-sail structure, which allows the structure to achieve different angles of rotation and provides with stable support by enlarging the supporting surface between the structure and the motor. Each generator in the turbine-sail structure is connected to a boost converter. An Arduino UNO is used as the controller. It receives commands from the upper computer (PC) and parses it to angles that the structure needs to rotate. Commands are processed in turn. The force sensor data during the rotation is returned and saved for data processing. A Graphical User Interface (GUI) is programmed to control experimental parameters on PC.

III. EXPERIMENT

A. Wind Tunnel Testbed and Experimental Setup

In order to test the proposed system, two sets of experiments are carried out in the wind tunnel in Harbin Institute of Technology, Shenzhen. The wind tunnel is 0.8m wide, 1m high and 5m long. The reflux wind tunnel supports wind speed ranging from 2m/s to 50m/s. The turbulence intensity is 0.5%. In experiments, the wind speed is set in a certain range (3.35m/s to 3.50m/s in the first set of experiments and 5.20m/s to 5.40m/s in the second set of experiments) and measured using a Pitot tube. The testbed is shown in Figure 6.

As shown in Figure 7, the experimental device (turbine-sail structure, thrust ball bearing, stepper motor, 3D force sensor) is placed in the wind tunnel. The wind is regarded as apparent wind in experiments, which is the wind experienced by a moving sailboat. The sail is in a downwind initial position (0°). The 3D force sensor is fixed in a direction that its X-channel axis has the same direction as the wind flow while the Y-channel axis is perpendicular to it. Since lift is the force generated perpendicular to the direction of the sailboat moving through the wind and drag is the force generated parallel to the direction of the sailboat moving through the wind in opposition, the X-channel axis force collected by the sensor is the drag in negative (denoted by F_D) and the Y-channel axis force is the lift (denoted by F_L). The turbine-sail structure will automatically rotate

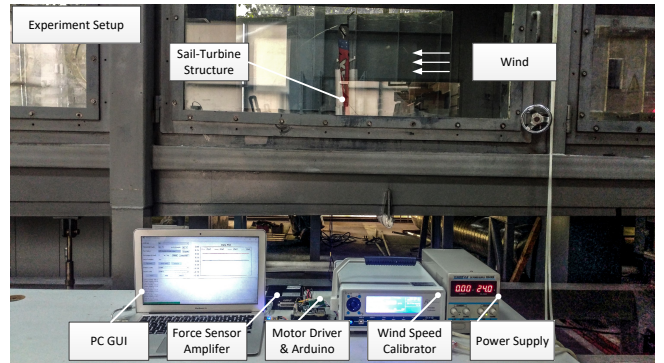


Fig. 6. Overview of wind tunnel testbed and experimental setup.

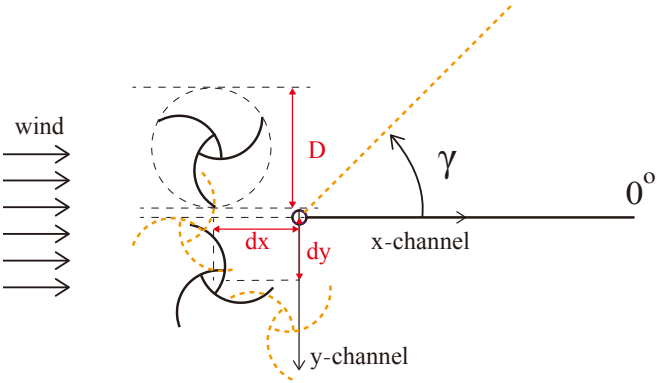


Fig. 7. Top view and parameter definition of the experimental system.

TABLE I
EXPERIMENTAL PARAMETERS.

Parameters	Values
Sail Height	51.5cm
Sail base line	13.5cm
D	50mm
dx	28mm
dy	28mm

in counterclockwise direction with small intervals of angle until it reaches 360° . As shown in Figure 7, D denotes the diameter of wind turbine blade's cross-section, d_x is the shortest distance from the vertical centerline of the mast to the connection of the center of the two wind turbines, d_y is the distance from the vertical shaft to the bisecting plane between two wind turbines. The experimental parameters are shown in Table I.

Given an imaginary course angle θ (see in Figure 8), the propulsive force F_P on boat can be calculated by:

$$F_P = F_{D\gamma} \cdot \cos \theta - F_{L\gamma} \cdot \sin \theta \quad (6)$$

where γ is the sail angle (as shown in Figure 7), and $F_{D\gamma}$, $F_{L\gamma}$ are the drag and lift at sail angle γ .

With the constant apparent wind, F_P under different sail angles γ in each imaginary course angle θ ($\theta = 0^\circ, 10^\circ, 20^\circ, 30^\circ, \dots, 360^\circ$) are calculated. Optimal sail angle for each θ is found to maximize the F_P . The maximum F_P , which can be denoted as $F_{P\max}$, is the largest propulsive force the boat can receive with a course angle θ .

In experiments, the 3D force sensor collect 1000 data sets of X-channel axis and Y-channel axis forces for each sail angle during the intermittent rotation. For example, if the rotation interval is 1.8° , both drag force and lift force have 201 data sets after one complete test. Mean value of each data set is correspondingly denoted as $\bar{F}_{D\gamma}$ or $\bar{F}_{L\gamma}$. For each course angle θ , the $F_{P\max}$ is expressed by Equation (7).

$$F_{P\max} = \max \{ \bar{F}_{D\gamma} \cos \theta - \bar{F}_{L\gamma} \sin \theta \}, \gamma \in [0^\circ, 360^\circ] \quad (7)$$

When the sail angle is around 0° and 180° , where the sail is almost parallel to the wind speed direction, the sail fluttered. Thus, the wind has little effect on the propulsion of the boat. The force data in these regions is relatively

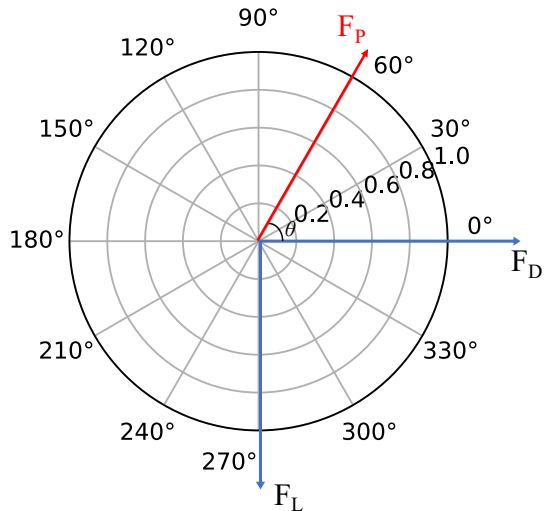


Fig. 8. Forces in polar coordinate with fixed $F_{D\gamma}$, $F_{L\gamma}$ positive directions.

unimportant. In order to improve the experimental efficiency on the premise of results accuracy, the upper device of the turbine-sail structure adopts irregular interval rotation instead of rotating regularly. The rotating intervals at different sail angle ranges are shown in Table II.

B. Experiments: with and without wind turbine blades

The aim of this set of experiments is to test whether the rotating wind turbine blades can increase the maximum propelling force under some course angles. The generators are not included in these experiments, so that the start-up torque of rotors is lower. The experiment therefore only requires small wind speed, ranging from 3.35m/s to 3.50m/s. Since each wind turbine can rotate either clockwise or counterclockwise, experiments are carried out at four rotating direction levels.

Also, experiments without wind turbine blades are conducted. For the non-blades group experiment, the vertical wind turbine blades are taken away from the upper experimental device, but the support frame is left. The $F_{P\max}$ values corresponding to course angle θ for different experiments are compared and the results are presented in Figure 9. The term to describe a sailing boat's course in relation to the wind direction is called points of sail. Some points of sail are not navigable (No-go zone in Figure 9). Some points of sail are navigable, but quite inefficiently (Don't-go zone in Figure 9) [15]. Don't-go zone is ignored in our data analysis. The results of $F_{P\max}$ value comparison between different levels of rotating direction in navigable regions are shown in Table III.

It can be observed from Figure 9 that adding vertical wind turbine blades will increase the maximum propelling force when sailing downwind (The downwind area is shown in Figure 9). Although the maximum propelling force generally decreases in the upwind area (The upwind area is shown in Figure 9), the system can still generate power as long as there is wind. And sailboats can move upwind in a zig-zag motion to avoid No-go zone. The results also indicate

TABLE II
ROTATING INTERVALS AT DIFFERENT SAIL ANGLE RANGES.

Sail Angle Range	$[0^\circ, 36^\circ]$	$[36^\circ, 129.6^\circ]$	$[129.6^\circ, 135^\circ]$	$[135^\circ, 225^\circ]$	$[225^\circ, 333^\circ]$	$[333^\circ, 360^\circ]$
Rotating Interval	9°	3.6°	5.4°	9°	5.4°	9°

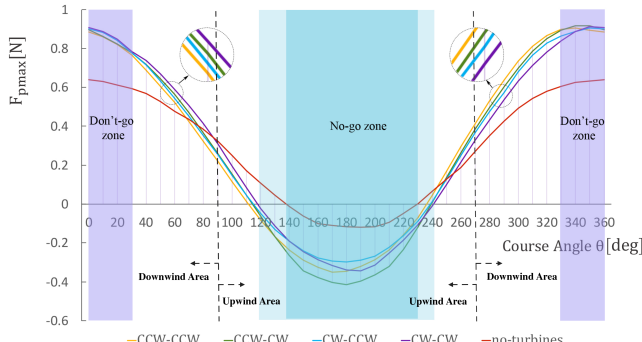


Fig. 9. Comparison between experiments with different directions of wind turbines rotation and non-turbine experiments. “CCW-CCW” denotes both turbines rotate in counterclockwise direction; “CCW-CW” denotes left-side (left-side presents the left-side of the sail from the wind direction) turbine rotates in counterclockwise direction and right-side (right-side presents the right-side of the sail from the wind direction) turbine rotates in clockwise direction; “CW-CCW” denotes left-side turbine rotates in clockwise direction and right-side turbine rotates in counterclockwise direction; “CW-CW” denotes both turbines rotate in clockwise direction.

TABLE III

$F_{P\max}$ VALUE COMPARISON BETWEEN 4 LEVELS OF ROTATING DIRECTION IN NAVIGABLE REGIONS.

Navigable Course Angle	$<180^\circ$	$>180^\circ$
$F_{P\max}$ from large to small	L: CW R: CW L: CCW R: CCW L: CCW R: CW L: CW R: CCW L: CCW R: CCW	L: CCW R: CCW L: CCW R: CW L: CW R: CCW L: CW R: CW

Notice: $<180^\circ$ represents navigable course angles that are less than 180° ; $>180^\circ$ represents navigable course angles that are larger than 180° .

that different rotation directions of wind turbines can affect the propulsion of sailboats seen in Table III. It suggests that it is feasible to control the rotation condition of wind turbines in different downwind course angles to obtain a larger maximum propelling force.

C. Experiments: with duty cycle adjustment

This set of experiments aims to test whether the maximum propelling force can be adjusted by changing the rotation speeds of wind turbines on both sides. The complete proposed structure is used in the experiments. Due to wind speed at which wind turbines start is higher than the cut-in speed, the wind speed in this set of experiments is controlled in a range from 5.20m/s to 5.40m/s. According to Table III, for course angles less than 180° , both wind turbines rotating in clockwise direction can obtain the largest maximum propelling force. Thus, in this set of experiments, we compare maximum propelling forces when course angles are less than 180° and both wind turbines rotate in clockwise

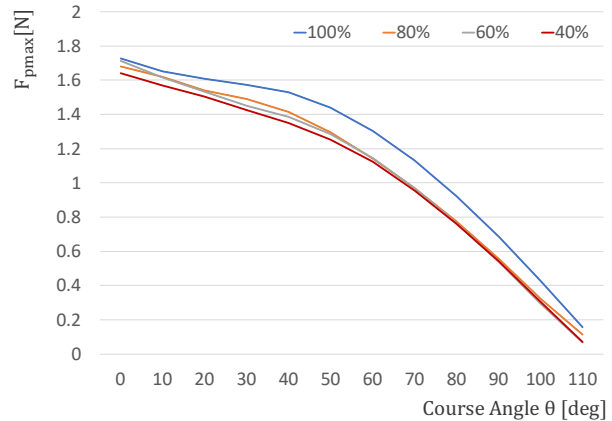


Fig. 10. Maximum propelling force curves with different duty cycle differences.

direction. During experiments, the duty cycle of boost converter that controls the right-side wind turbine is always 0%, which results in full speed rotation. The duty cycle of the boost converter that controls the left-side wind turbine is adjusted to be 100%, 80%, 60% and 40% in corresponding experiments. The rotation speed increases as the duty cycle decreases.

Figure 10 shows the experiment results with different duty cycle differences between left-side and right-side boost converters. When the duty cycle difference reaches the maximum value 100%, the maximum propelling force is also the largest compared with the other three curves. The maximum propelling force generally decreases when the duty cycle difference decreases. When the duty cycle difference reaches 40%, the values of maximum propelling force curve are the smallest among all these curves.

Therefore, the experimental results show that the maximum propelling force can be increased by slowing the rotation speed of wind turbine on one side in navigable downwind course angle range. Combined with the results from Section III-B, these experiments show that the proposed turbine-sail system can utilize wind energy not only by generating power but also by increasing the maximum downwind propelling force in an adjustable way. A balance between generating power and increasing downwind propelling force can be reached depending on practical needs.

IV. CONCLUSION

In this paper, a new turbine-sail coupled propulsive system is proposed for autonomous sailboat to utilize wind power for generating electric power and increasing its maximum propelling force. The proposed turbinesail structure contains two vertical wind turbines, which

rotation speed can be adjusted using boost converters, so that this system can generate power and regulate the maximum propelling force for sailboats. The experiments show that by adding such vertical wind turbines, their blades will increase the maximum propelling force when sailing downwind with navigable course angles. In this course angle range, adjustments that increase the rotation speed difference between two wind turbines can increase the maximum propelling force. This brings positive effects on some aspects in the study of autonomous sailboats, such as the flexibility of unmanned sailboats, the efficiency of missions and the long-distance navigation power strategy.

In future works, the turbine-sail structure will be deployed on an autonomous sailboat for experimental measurements in real scenes to test its actual effect. More potential practical uses will be explored through such real scene experiments.

REFERENCES

- [1] Z. Liu, Y. Zhang, X. Yu, and C. Yuan, "Unmanned surface vehicles: An overview of developments and challenges," *Annual Reviews in Control*, vol. 41, pp. 71–93, 2016.
- [2] R.-j. Yan, S. Pang, H.-b. Sun, and Y.-j. Pang, "Development and missions of unmanned surface vehicle," *Journal of Marine Science and Application*, vol. 9, no. 4, pp. 451–457, 2010.
- [3] Z. Yuyi, Z. Yu, L. Huanxin, L. Yunjia, and L. Liang, "Control system design for a surface cleaning robot," *International Journal of Advanced Robotic Systems*, vol. 10, no. 5, p. 220, 2013.
- [4] R. R. Murphy, E. Steimle, C. Griffin, C. Cullins, M. Hall, and K. Pratt, "Cooperative use of unmanned sea surface and micro aerial vehicles at hurricane wilma," *Journal of Field Robotics*, vol. 25, no. 3, pp. 164–180, 2008.
- [5] Y. Ma, Y. Zhao, J. Diao, L. Gan, H. Bi, and J. Zhao, "Design of sail-assisted unmanned surface vehicle intelligent control system," *Mathematical Problems in Engineering*, vol. 2016, 2016.
- [6] D. Santos, A. Silva Junior, A. Negreiros, J. Vilas Boas, J. Alvarez, A. Araujo, R. Aroca, and L. Gonçalves, "Design and implementation of a control system for a sailboat robot," *Robotics*, vol. 5, no. 1, p. 5, 2016.
- [7] C. Viel, U. Vautier, J. Wan, and L. Jaulin, "Position keeping control of an autonomous sailboat," *IFAC-PapersOnLine*, vol. 51, no. 29, pp. 14–19, 2018.
- [8] J. Melin, K. Dahl, and M. Waller, "Modeling and control for an autonomous sailboat: a case study," in *World Robotic Sailing championship and International Robotic Sailing Conference*. Springer, 2015, pp. 137–149.
- [9] H. Saoud, M.-D. Hua, F. Plumet, and F. B. Amar, "Routing and course control of an autonomous sailboat," in *2015 European Conference on Mobile Robots (ECMR)*. IEEE, 2015, pp. 1–6.
- [10] B. Clement, "Control algorithms for a sailboat robot with a sea experiment," *IFAC Proceedings Volumes*, vol. 46, no. 33, pp. 19–24, 2013.
- [11] F. Plumet, C. Pêtrès, M.-A. Romero-Ramirez, B. Gas, and S.-H. Ieng, "Toward an autonomous sailing boat," *IEEE Journal of Oceanic Engineering*, vol. 40, no. 2, pp. 397–407, 2014.
- [12] V. Alfonsín, A. Suárez, A. Cancela, A. Sanchez, and R. Maceiras, "Modelization of hybrid systems with hydrogen and renewable energy oriented to electric propulsion in sailboats," *international journal of hydrogen energy*, vol. 39, no. 22, pp. 11 763–11 773, 2014.
- [13] M. Zemamou, M. Aggour, and A. Toumi, "Review of savonius wind turbine design and performance," *Energy Procedia*, vol. 141, pp. 383–388, 2017.
- [14] X. Liang, S. Fu, B. Ou, C. Wu, C. Y. Chao, and K. Pi, "A computational study of the effects of the radius ratio and attachment angle on the performance of a darrieus-savonius combined wind turbine," *Renewable energy*, vol. 113, pp. 329–334, 2017.
- [15] R. Stelzer, T. Proll, and R. I. John, "Fuzzy logic control system for autonomous sailboats," in *2007 IEEE International Fuzzy Systems Conference*. IEEE, 2007, pp. 1–6.